



**AN EXPLICIT MODEL OF THE MOS TRANSISTOR
FOR DESIGN AND SIMULATION OF ANALOG CIRCUITS**

Ana Isabela Araújo Cunha*, Márcio Cherem Schneider and Carlos Galup-Montoro
Laboratório de Instrumentação Eletrônica - Departamento de Engenharia Elétrica
Universidade Federal de Santa Catarina - C. P. 476
88 040 900 - Florianópolis - SC - Brasil
Telephone: 55-482 31-9643 Fax: 55-482 31-9770
E-mail: carlos@linse.ufsc.br

Abstract - This paper presents an explicit analytical model of the long-channel MOS transistor valid in all regions of operation - weak, moderate and strong inversion. The drain current, total charges and small-signal parameters for quasi-static operation are expressed as very simple functions of the inversion charge densities at the channel ends. The charge densities, in turn, are formulated as explicit continuous functions of the terminal voltages, with continuous first order derivatives. The proposed model is precise and very simple to be incorporated in CAD programs or to be used in designs by hand. Moreover, our model contains only the classical parameters of the MOSFET theory.

(*) On leave from Departamento de Engenharia Elétrica, Escola Politécnica, Universidade Federal da Bahia, CEP 40210-630, Salvador, BA, Brasil.



I - Introduction

Despite the existence of several MOSFET models, none of them includes simple formulae to describe adequately the transistor characteristics in all operating regions [1]. Models based on the classical linear approximation of the inversion charge density in strong inversion are often used in CAD programs. Nevertheless, they do not express satisfactorily the MOSFET behavior [2], mainly in the so-called "moderate inversion region".

This paper presents an explicit model of the long-channel MOS transistor valid in all regions of operation. Our model is based on an approximation of the semiconductor capacitance [3], which allows determining an explicit expression for the inversion charge density in terms of the terminal voltages. The MOSFET static and dynamic characteristics have an explicit formulation in terms of the inversion charge densities at the source and drain ends.

II - Approximation of the Semiconductor Capacitance

Our model is based on an approximation of the semiconductor capacitance per unit area, C'_s , in inversion. This capacitance is usually split into two components [1], the inversion (C'_i) and depletion (C'_b) capacitances:

$$C'_s = C'_i + C'_b, \quad (1)$$

which we have written as functions of the inversion (Q'_i) and depletion (Q'_b) charge densities:

$$C'_i = \frac{|Q'_i|}{2\phi_t} \left(1 + \frac{Q'_b}{Q'_c} \right) \quad (2.a)$$

$$C'_b = \frac{\gamma^2 C'_{ox}{}^2}{2|Q'_c|} \quad (2.b)$$

Here ϕ_t is the thermal voltage, C'_{ox} is the oxide capacitance per unit area, γ is the body effect factor and Q'_c is the semiconductor charge density given by:

$$Q'_c = Q'_i + Q'_b \quad (2.c)$$



Eqn.(2.a) allows achieving an explicit formulation of the inversion capacitance from conventional approximations of the semiconductor charges. We use here the linear function of the channel potential V_{CB} , valid in strong inversion:

$$-Q'_i = C'_{ox} n (V_p - V_{CB}) - Q'_{IP} \quad \text{for } V_{CB} \leq V_p \quad (3.a)$$

Q'_{IP} is the value of the inversion charge density in the upper limit of weak inversion which has been included in the formula presented in refs.[4, 5] in order to obtain a continuous transition for Q'_i , from strong to weak inversion. In eqn.(3.a), V_p (Table 2) is the pinch-off voltage [4, 5] that can be approximated by [5]

$$V_p \cong \frac{V_{CB} - V_{T0}}{n} \quad (3.b)$$

where V_{T0} is the value of the threshold voltage for $V_{CB} = 0$ and n (Table 2) is the slope factor.

Substituting eqn.(3.a) into eqn.(2.a), we approximate the inversion capacitance in strong inversion, including the so-called moderate inversion region, by:

$$C'_i = \frac{C'_{ox}}{2\phi_t} n (V_p - V_{CB}) \left(1 + \frac{Q'_B}{Q'_C} \right) - \frac{Q'_{IP}}{2\phi_t} \left(1 + \frac{Q'_B}{Q'_C} \right) \quad \text{for } V_{CB} \leq V_p \quad (4)$$

The first term in the right hand side of eqn.(4) prevails deep in strong inversion, where the term $1+Q'_B/Q'_C$ can be approximated to 1. The second term predominates near threshold, where the term $1+Q'_B/Q'_C$ can be better approximated to 2. Assuming that in strong inversion $C'_i \cong C'_s$, we can, therefore, write:

$$C'_i \cong C'_s \cong C'_{ox} n \frac{(V_p - V_{CB})}{2\phi_t} + (n-1)C'_{ox} \quad , \quad \text{for } V_{CB} \leq V_p \quad (5.a)$$

which is a slight modification of the semiconductor capacitance model used in ref.[3] to determine the harmonic distortion in MOS gate capacitors in strong inversion. Eqn.(5.a) represents the fundamental approximation to be used throughout this work in order to achieve explicit expressions that represent the static and dynamic behavior of the MOS transistor. The term $(n-1)C'_{ox}$ guarantees continuity between eqn.(5.a) and the classical approximation of the semiconductor capacitance in weak inversion:

$$C'_i \cong C'_b \cong \frac{\gamma}{2\sqrt{2\phi_f + V_p}} C'_{ox} = (n-1)C'_{ox} \quad \text{for } V_{CB} \geq V_p \quad (5.b)$$



Fig.1 shows the values of the gate capacitance (C'_g),

$$\frac{1}{C'_g} = \frac{1}{C'_c} + \frac{1}{C'_{ox}}, \quad (6)$$

computed from the explicit expression of the semiconductor capacitance, eqns.(5), from the theoretical implicit expression of C'_c [1] and from the usual approximation assuming infinite semiconductor capacitance for strong inversion.

III - Approximation of the Inversion Charge Density

The inversion charge density Q'_i can be determined from:

$$Q'_i = Q'_{fp} + \int_{V_p}^{V_{cb}} \frac{dQ'_i}{dV_{cb}} dV_{cb} \quad (7.a)$$

where

$$\frac{dQ'_i}{dV_{cb}} = \left(1 + \frac{\gamma}{2\sqrt{\phi_s}} \right) \frac{C'_i}{1 + C'_c/C'_{ox}} \quad (7.b)$$

and ϕ_s is the surface potential.

Substituting eqn.(7.b) into eqn.(7.a) and approximating ϕ_s by its value $2\phi_f + V_p$ at pinch-off, we obtain:

$$Q'_i = Q'_{fp} + n \int_{V_p}^{V_{cb}} \frac{C'_i}{1 + C'_c/C'_{ox}} dV_{cb} \quad (7.c)$$

In order to evaluate the integral in eqn.(7.c) we have used the strong inversion approximation of C'_c and C'_i given by eqn.(5.a), which leads to the expression of Q'_i presented in Table 1. For weak inversion, we have adopted here the conventional expression for the inversion charge density [1, 4, 5], also presented in Table 1.

The expressions of Q'_i in Table 1, in weak and strong inversion, represent a piecewise but smooth function. They provide a continuous transition from weak to strong inversion as well as from conduction to saturation for Q'_i and its first order partial derivatives with respect to V_{GB} and V_{CB} (Table 1).



IV - Drain Current and Total Charges

A linearization of $Q'_i(\phi_s)$ about $2\phi_F + V_p$ gives:

$$\frac{dQ'_i}{d\phi_s} = nC'_{ox} \quad (8)$$

The use of eqn.(8) allows changing the variable ϕ_s to Q'_i in the integral expression of the drain current [1]:

$$I_D = -\frac{\mu}{nC'_{ox}} \frac{W}{L} \int_{Q'_B}^{Q'_D} (Q'_i - nC'_{ox}\phi_s) dQ'_i \quad (9)$$

where Q'_B and Q'_D are the inversion charge densities at the source and drain ends, respectively, μ is the carrier mobility, W is the channel width and L is the channel length.

By means of the additional change of variable that follows,

$$Q'_h = Q'_i - nC'_{ox}\phi_s, \quad (10)$$

eqn.(9) becomes:

$$I_D = -\frac{\mu}{nC'_{ox}} \frac{W}{L} \int_{Q'_F}^{Q'_R} Q'_h dQ'_h = \frac{\mu}{C'_{ox}} \frac{W}{L} \frac{Q'_F{}^2 - Q'_R{}^2}{2n} \quad (11)$$

where Q'_F and Q'_R are the values of Q'_h evaluated at the source and drain ends, respectively (Table 2). In Fig.2, the current computed from eqn.(11), together with the approximation of Q'_i given in Table 1, is compared to that evaluated from the Brews model [1].

Through an analogous procedure, we find the total inversion (Q_i) and depletion (Q_B) charges:

$$Q_i = WL \left[\frac{2 Q'_F{}^2 + Q'_F Q'_R + Q'_R{}^2}{3(Q'_F + Q'_R)} + nC'_{ox}\phi_s \right] \quad (12.a)$$

$$Q_B = Q_p - \frac{n-1}{n} Q_i \quad (12.b)$$

where

$$Q_p = WL \left[Q'_{BP} + \frac{n-1}{n} Q'_{FP} \right] \quad (12.c)$$

and

$$Q'_{BP} = -C'_{ox}\gamma \sqrt{2\phi_F + V_p} \quad (12.d)$$



V - Small-Signal Parameters

The MOSFET intrinsic capacitances for quasi-static operation can be evaluated by differentiating the expressions of the total charges derived in the previous Section. The results are presented in Table 3.

In order to obtain the MOSFET source, drain and gate transconductances we have adopted the expression [1]:

$$I_D = \mu \frac{W}{L} \int_{V_{DS}}^{V_{DB}} (-Q'_i) dV_{CB} \quad (13)$$

Differentiating eqn.(13) with respect to the terminal voltages, we find the expressions for the transconductances presented in Table 3.

We have used the relationship

$$\left. \frac{\partial Q'_i}{\partial V_G} \right|_{V_C, V_B} \equiv -\frac{1}{n} \left. \frac{\partial Q'_i}{\partial V_C} \right|_{V_G, V_B} \quad (14)$$

to derive the expressions for C_{gs} and g_{mG} . Eqn.(14) follows directly from the expressions of Q'_i in Table 1 for both strong and weak inversion if we assume that the variation of n with V_{CB} is negligible [4, 5].

The MOSFET small-signal parameters (Fig.3) are represented by simple and symmetric expressions that are accurate explicit functions of the terminal voltages if the inversion charge density and its derivatives are evaluated at drain and source according to the expressions derived in Section III. Tables 1, 2 and 3 summarize the formulae of the proposed model.

VI - Conclusions

We have accomplished a general explicit model very appropriate for the simulation of MOSFET circuits since the needs for simplicity and accuracy are simultaneously fulfilled. A smooth variation of the MOSFET characteristics, including small signal parameters, is



guaranteed through the entire inversion region (weak, moderate and strong inversion). Moreover, our model contains only the classical parameters of the MOSFET theory.

REFERENCES

- [1] Tsividis, Y. **"Operation and modeling of the MOS transistor"**, McGraw-Hill, New York, 1987.
- [2] Tsividis, Y. and Masetti, G. **"Problems in precision modeling of the MOS transistor for analog applications"**, *IEEE Transactions on Computer Aided Design*, vol. 3, N° 1, January 1984, pp. 72-79.
- [3] Behr, A.T., Schneider, M.C., Noceti Filho, S. and Galup-Montoro, C. **"Harmonic distortion caused by capacitors implemented with MOSFET gates"**, *IEEE Journal of Solid-State Circuits*, vol. 27, N° 10, October 1992, pp. 1470-1475.
- [4] Enz, C. **"High-precision CMOS micropower amplifiers"**, Ph-D. Thesis N° 802, EPF-Lausanne, 1989.
- [5] Vittoz, E. **"Intensive summer course on CMOS VLSI design - Analog & Digital"**, EPF-Lausanne, 1989.

Definitions and technological parameters regarding the figures:

$$u_{GB} = \frac{V_{GB}}{\phi_t} \quad u_{CB} = \frac{V_{CB}}{\phi_t} \quad u_{SB} = \frac{V_{SB}}{\phi_t} \quad u_{DB} = \frac{V_{DB}}{\phi_t} \quad u_{FB} = \frac{V_{FB}}{\phi_t} \quad u_{T0} = \frac{V_{T0}}{\phi_t}$$

$$I_0 = \frac{\mu W}{L} C_{ox} \phi_t^2 \quad g_0 = \frac{\mu W}{L} C_{ox} \phi_t$$

$$N_A = 5 \times 10^{15} \text{ cm}^{-3} \quad t_{ox} = 878 \text{ \AA} \quad V_{FB} = -1.18 \text{ V}$$

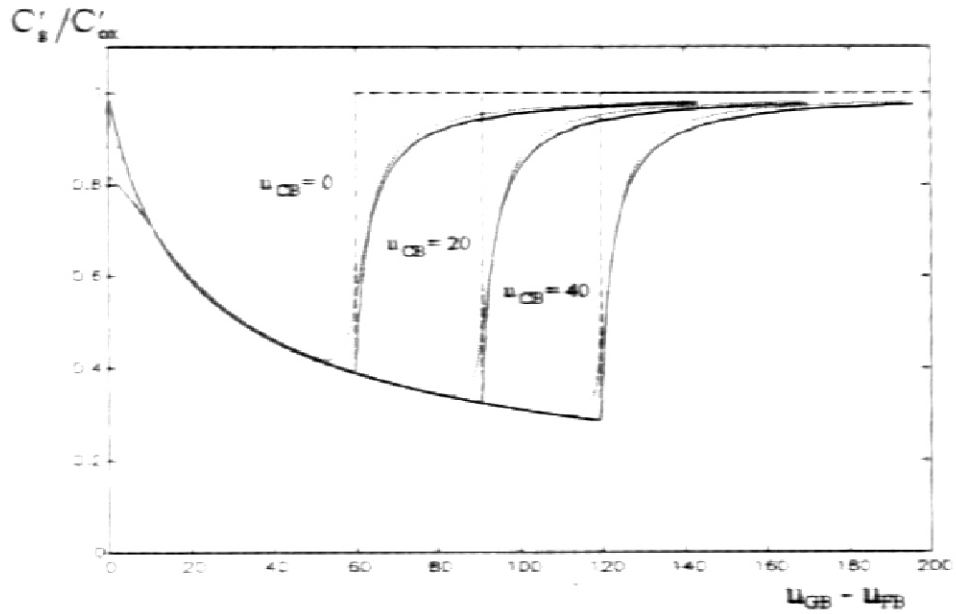


Fig. 1. Normalized gate capacitance per unit area versus normalized gate voltage computed from:

- _____ Our model
- The theoretical implicit expression [1]
- The conventional model (infinite semiconductor capacitance in strong inversion)

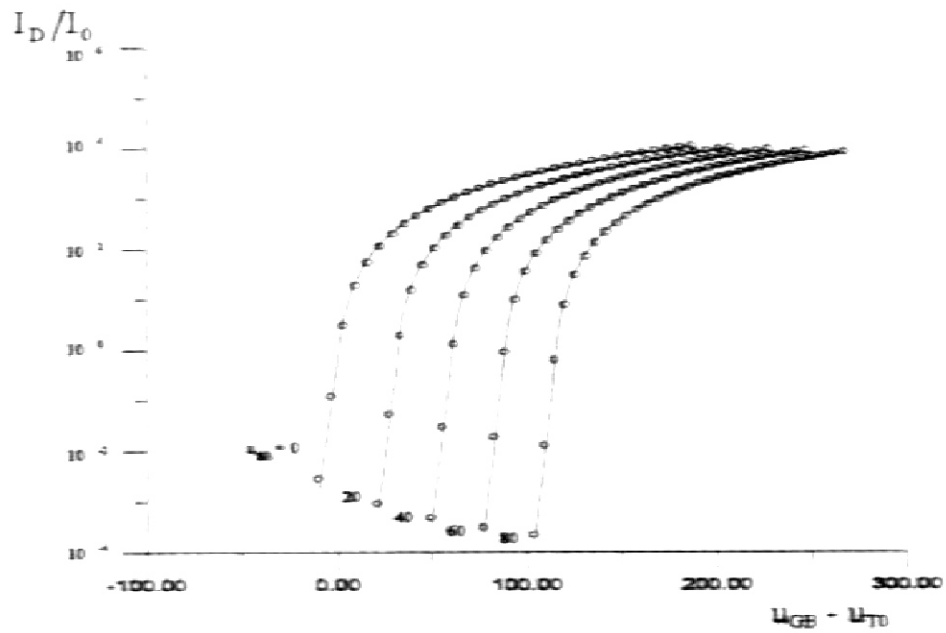


Fig. 2. Normalized drain current in saturation versus normalized gate voltage computed from:

- _____ Our model - Table 1
- o o o o o The charge-sheet model [1]

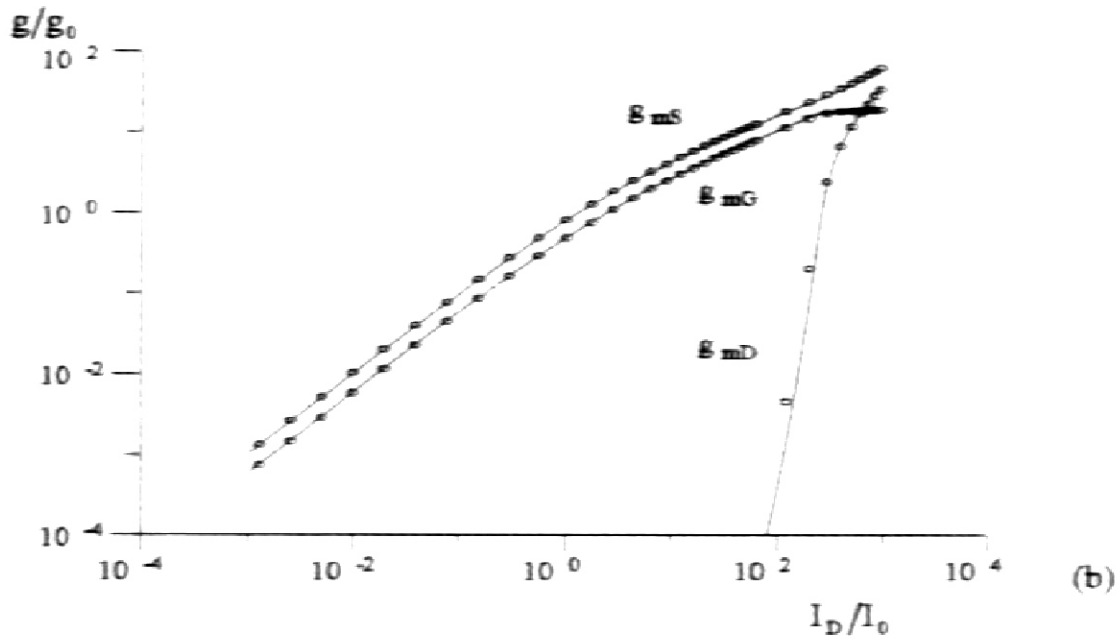
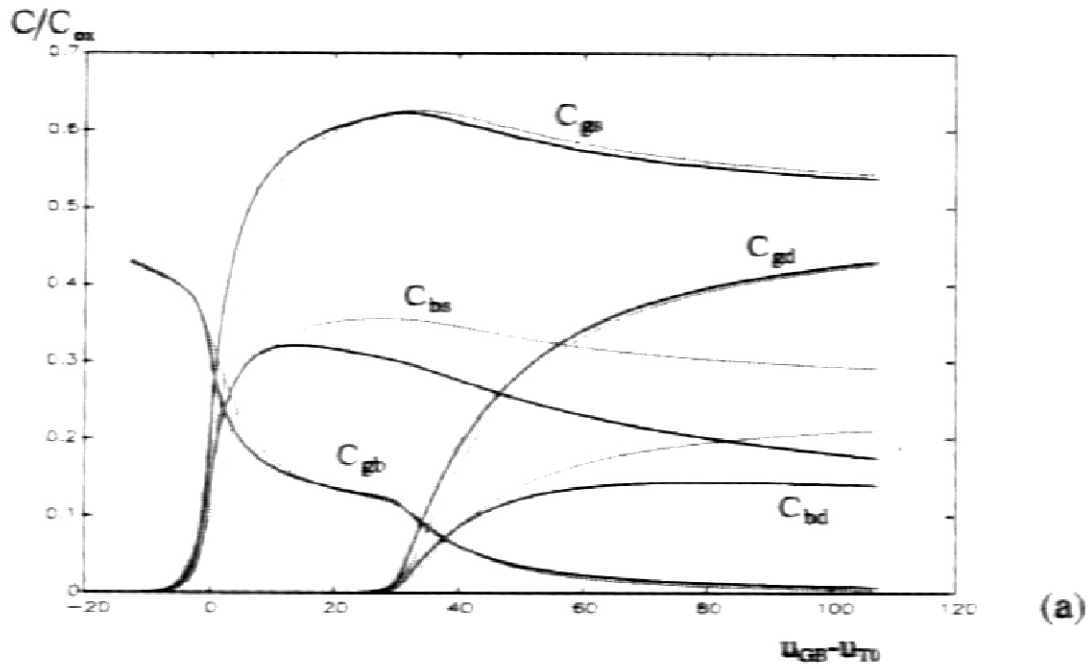


Fig.3. Normalized small-signal parameters for $u_{GS} = 0$ and $u_{DS} = 20$

(a) Intrinsic capacitances versus normalized gate-to-source voltage

(b) Transconductances versus normalized drain current

_____ Our model

..... or o o o o o Charge sheet model



Table 1 - Inversion Charge Density (Q'_i) and Its Derivative (D') with respect to V_{CB}

| Quantity | Expression | |
|------------------------|---|---|
| | $V_{CB} \geq V_p$ (weak inversion) | $V_{CB} \leq V_p$ (strong inversion) |
| $Q'_i(V_{CB}, V_{GB})$ | $-C'_{ox}(n-1)\phi_i e^{(V_p - V_{CB})/\phi_i}$ | $-C'_{ox} \left[n(V_p - V_{CB}) - 2\phi_i \ln \left(1 + \frac{V_p - V_{CB}}{2\phi_i} \right) + (n-1)\phi_i \right]$ |
| $D'(V_{CB}, V_{GB})$ | $-Q'_i(V_{CB}, V_{GB})/\phi_i$ | $C'_{ox} \left[n - \left(1 + \frac{V_p - V_{CB}}{2\phi_i} \right)^{-1} \right]$ |

Table 2 - Auxiliary Functions and Parameters

| Quantity | Expression | Quantity | Expression | Quantity | Expression |
|----------|---|----------|--------------------------|----------|---|
| Q'_F | $Q'_i(V_{GB}, V_{GB}) - nC'_{ox}\phi_i$ | A | $\frac{2}{3}WL$ | n | $1 + \frac{\gamma}{2\sqrt{2\phi_F + V_p}}$ |
| D'_F | $D'(V_{GB}, V_{GB})$ | B | $\frac{\mu W}{C'_{ox}L}$ | V_p | $\left(\sqrt{V_{GB} - V_{FB} + \frac{\gamma^2}{4}} - \frac{\gamma}{2} \right)^2 - 2\phi_F$ |
| Q'_R | $Q'_i(V_{DB}, V_{GB}) - nC'_{ox}\phi_i$ | | | | |
| D'_R | $D'(V_{DB}, V_{GB})$ | | | | |

Table 3 - Drain Current and Small Signal Parameters

| Quantity | Expression | Quantity | Expression | Quantity | Expression |
|----------|--|----------|--|----------|---|
| I_D | $B \frac{(Q'^2_F - Q'^2_R)}{2n}$ | B_{ns} | $-BC'_{ox}(Q'_F + nC'_{ox}\phi_i)$ | B_{nd} | $-BC'_{ox}(Q'_R + nC'_{ox}\phi_i)$ |
| C_{gs} | $\frac{A}{n} \left[1 - \frac{Q'^2_R}{(Q'_F + Q'_R)^2} \right] D'_F$ | C_{gd} | $\frac{A}{n} \left[1 - \frac{Q'^2_F}{(Q'_F + Q'_R)^2} \right] D'_R$ | C_{gs} | $\frac{n-1}{n}(C_{ox} - C_{gs} - C_{gd})$ |
| C_{gd} | $(n-1)C_{gs}$ | C_{nd} | $(n-1)C_{gd}$ | B_{ng} | $\frac{B_{ns} - B_{nd}}{n}$ |